

Appendix IV

NRC Staff Computational Fluid Dynamics Simulations in Support of the SONGS Audit

The San Onofre Nuclear Generating Station (SONGS) licensee performed computational fluid dynamics (CFD) simulations with the FLOW-3D code that were used as an input to its debris transport analysis [1]. The licensee considered two CFD cases, a large break on the Loop 1 hot leg (Case 1) and a large break on the Loop 2 hot leg (Case 2). The licensee provided FLOW-3D input decks for these two cases for the staff to review during the audit.

In order to assess the conservatism of the licensee's debris transport results, the NRC staff performed a series of sensitivity simulations based on the two CFD input decks provided by the licensee. The purpose of the sensitivity simulations was to provide assurance that the two CFD simulations performed by the licensee acceptably bound the range of potential debris transport conditions that may be expected for SONGS during sump recirculation. Therefore, in performing the sensitivity simulations, the staff varied parameters in the as-received CFD input decks that were considered to be significant in order to determine whether plausible perturbations to the CFD model would affect containment pool flow parameters of interest to debris transport, such as velocity and turbulence. This appendix describes the results of the staff's simulations. Additional information concerning the licensee's debris transport analysis and the staff's review thereof is provided in Section 3.5 of the main report.

In conducting the CFD sensitivity simulations, the staff generally focused upon the Case 1 break because the licensee determined that this break was limiting with respect to debris transport. However, simulations were conducted for the Case 2 break as well to assess the licensee's conclusion that this break was bounded. The various sensitivity simulations conducted by the staff are listed in Table 1.

Each of the following sections of this appendix describes one of the staff's sensitivity simulations, providing (1) a brief rationale for conducting the simulation, (2) a figure showing a plot of the resulting containment pool velocity magnitude contours on a horizontal plane just above the containment floor, and (3) a brief analysis of the results of the simulation.

All of the figures showing the containment pool velocity magnitude contour plots use a velocity scale from 0 to 0.16 ft/s. The upper velocity limit of 0.16 ft/s was chosen because this velocity corresponds to the tumbling velocity transport metric for small pieces of mineral wool. Since mineral wool is the primary source of fibrous debris at SONGS, analyzing its transport behavior is of particular importance to ensuring that the replacement strainer design is adequate. As noted above, all of the velocity plots in this appendix depict a horizontal plane just above the containment floor. Based upon the meshing employed in the as-received input decks, the height of this plane is 2 inches above the floor level (i.e., at the center of the first layer of 4-inch-high cells) for all sensitivity cases except the increased mesh resolution case (Case 1-7), which is discussed in detail below.

Finally, in addition to the sensitivity cases that were performed based upon the licensee's input decks, the staff also conducted a simplified simulation of containment spray drainage that will be discussed briefly at the end of this appendix.

Table 1: NRC Staff CFD Sensitivity Simulations

Case	Description
Case 1 Break Simulations	
1-1	Baseline Case
1-2	Reduced Pool Temperature Case
1-3	Southeast Passage Blockage Case
1-4	Elimination of Containment Spray Alternating Horizontal Velocity Component Case
1-5	Increased Containment Spray Flow Case
1-6	Increased Refueling Canal Drainage Flow Case
1-7	Increased Mesh Resolution Case
1-8	Extended Simulation Time Case
Case 2 Break Simulations	
2-1	Elimination of Containment Spray Alternating Horizontal Velocity Component Case
2-2	Southeast Passage Blockage Case
2-3	Southeast Passage Blockage Plus Increased Refueling Canal Drainage Flow Case

Case 1-1: Baseline Case

Upon obtaining the FLOW-3D input decks from the licensee, the staff desired to run the as-received Case 1 input deck to generate results that could be directly compared to the licensee's CFD results presented in the debris transport calculation [1]. While several formatting changes to the input deck were necessary for compatibility with the staff's workstation, no modifications were made to the computational model. Figure 1 shows the plot of velocity magnitude contours generated from the as-received Case 1 input deck.

For clarity, labels are provided on Figure 1 for the break location, the refueling canal drain line, and the recirculation sumps. Although velocity vectors are not provided on Figure 1 or the following figures in an effort to preserve clarity, several arrows have been manually added to Figure 1 to highlight the general containment flow pattern. These arrows are not vectors because their length has not been scaled based upon the local velocity of the flow. Note that the containment pool flow generally proceeds from the break location and refueling canal drain toward the recirculation sumps, although several of the flowpaths to the sump appear somewhat circuitous. Since the locations of interest and general flow pattern shown on Figure 1 are very similar (or identical) for all Case 1 simulations, labels and arrows are not provided on succeeding Case 1 figures.

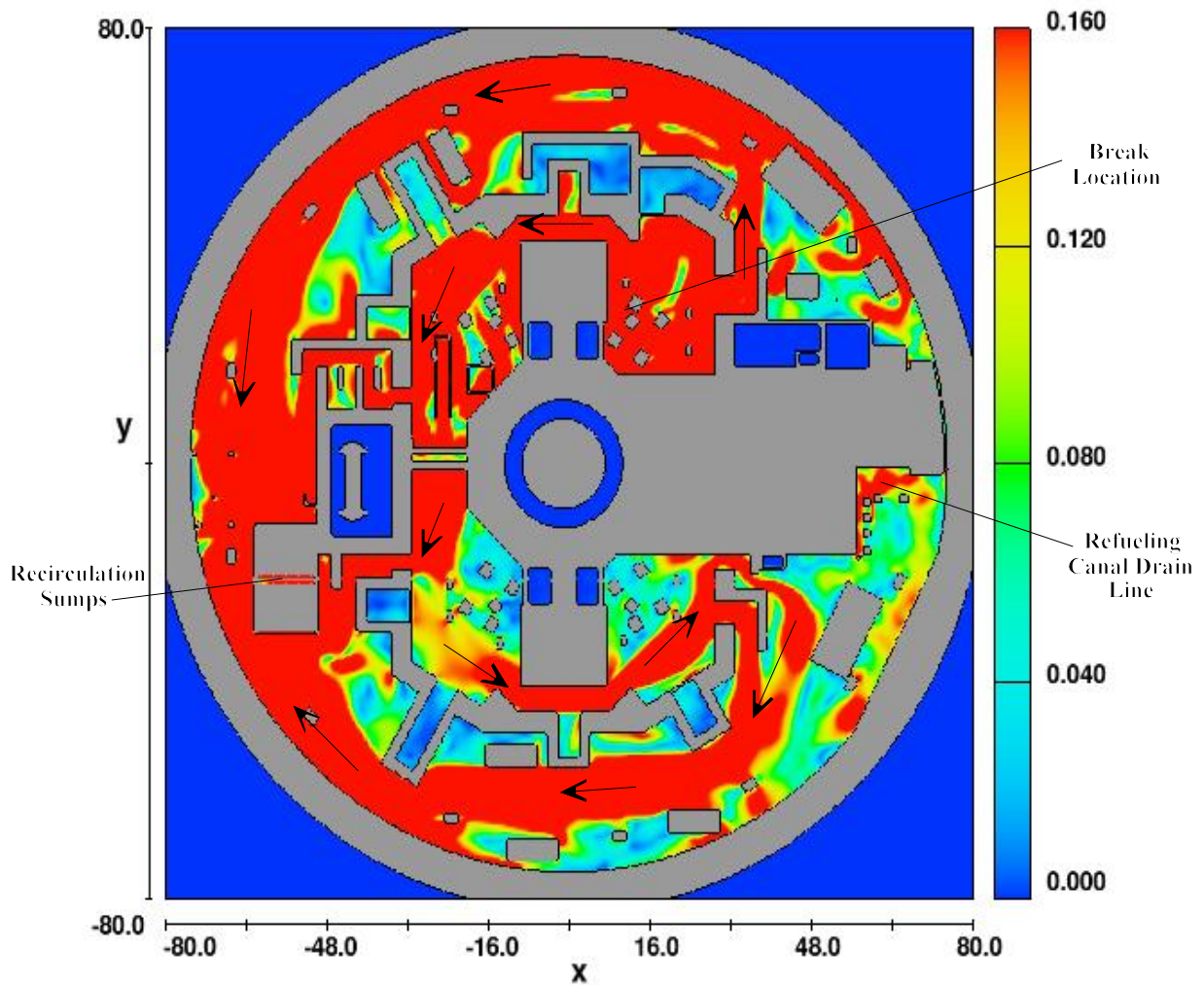


**Figure 1: Baseline Case
Containment Pool Velocity [ft/s]**

The staff observed that Figure 1 corresponds closely to the analogous figure the licensee generated for Case 1 in the debris transport calculation (Figure 5.9.11) [1]. While this result is expected based upon the fact that no substantial changes were made to the input deck, it confirms that the licensee's results can be essentially replicated on a different computational platform.

Figures 2 and 3 plot the estimated mean kinetic energy and average turbulent kinetic energy versus time predicted by the FLOW-3D code for the baseline simulation. These plots show that the mean kinetic energy and average turbulent kinetic energy have essentially stabilized by the end of the simulation. The licensee used a mean kinetic energy versus time plot similar to Figure 2 to determine that its CFD simulations had reached a steady state. In discussing Case 1-8, the staff will show that this approach may not be sufficient to ensure that all local flow developments of significance to the overall debris transport results have stabilized.

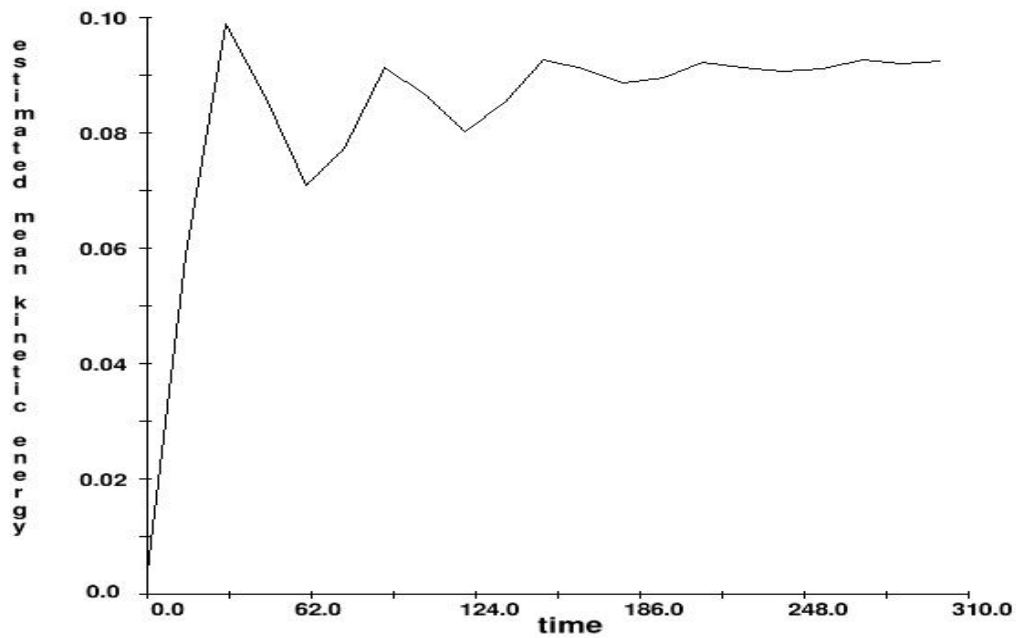


**Figure 2: Baseline Case Estimated Mean Kinetic Energy [ft²/s²]
Versus Simulation Time [s]**

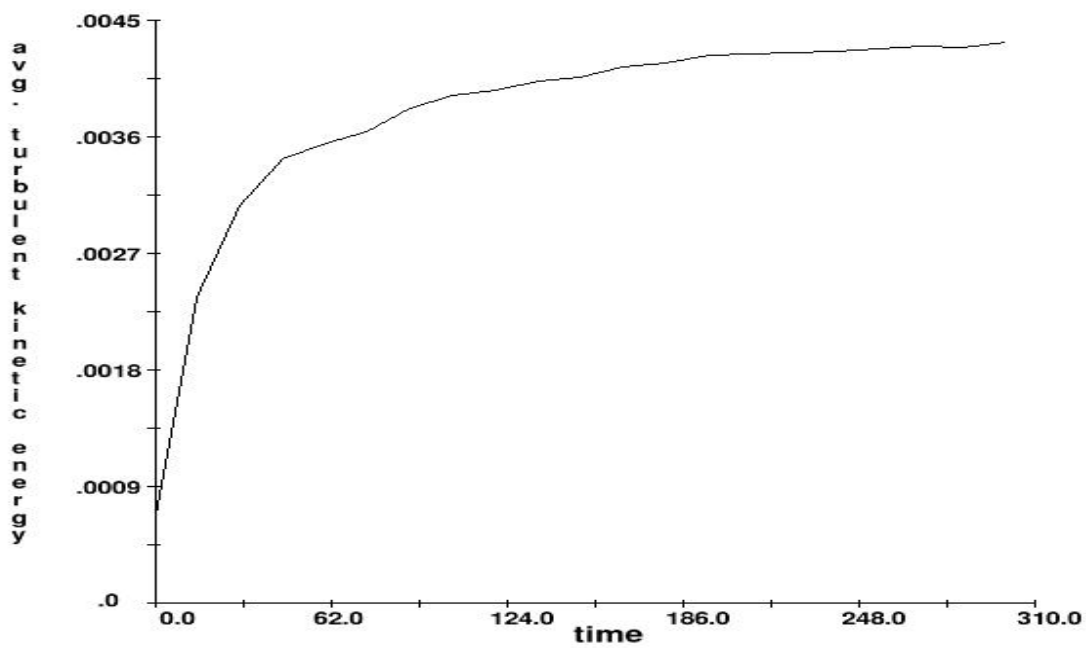


**Figure 3: Baseline Case Average Turbulent Kinetic Energy [ft²/s²]
Versus Simulation Time [s]**

Case 1-2: Reduced Pool Temperature Case

Both of the licensee's CFD cases used a containment pool temperature of 212°F [1]. The licensee stated that 212°F is very close to the maximum containment pool temperature calculated to exist at the beginning of sump recirculation (215°F) [1]. The licensee further stated that a slight temperature variation would have a negligible effect on the CFD results, based upon previous simulations showing that a containment pool at 250°F would have only a slightly higher transport capability than the same pool at 100°F [1].

The staff considered 212°F to be essentially indistinguishable from 215°F with respect to computing the containment pool flow field as an input to the debris transport analysis. However, the staff desired to confirm the licensee's observation that larger temperature differences would not significantly impact the CFD results in order to examine the applicability of the calculated transport results at reduced containment pool temperatures. Therefore, the staff altered the baseline CFD input deck to simulate a pool temperature of 120°F and performed a CFD run using this revised deck for 300 seconds of simulated time. A plot of the resulting velocity magnitude contours is presented as Figure 4.

No significant differences were observed from a comparison of the results of the Reduced Temperature Case (Figure 4) to the Baseline Case (Figure 1). The few subtle differences between the two cases may result from fluctuations in the code predictions on the approach to a steady-state solution. The results of the reduced temperature simulation indicate that, barring changes to the physical properties of the debris in the containment pool, the debris transport results are not likely to change significantly as the result of expected changes in fluid temperature and temperature-dependent fluid parameters such as viscosity.

Case 1-3: Southeast Passage Blockage Case

The staff performed a CFD sensitivity simulation to address the potential for blockage to occur at one of the two passages in the southeast corner of the Loop 2 steam generator compartment. In a discussion of potential water hold up points in the debris transport calculation, the licensee indicated that a heating, ventilating, and air conditioning (HVAC) plenum is located in this passage, which poses the potential for blocking flow [1]. The licensee did not model this blockage in its input decks based upon engineering judgment that the presence of another open passageway in the same general location would preclude significant changes to the CFD simulation results [1].

To assess the validity of the licensee's conclusion, the staff explicitly modeled blockage at the affected passage in the southeast corner of the Loop 2 steam generator compartment. To implement this model, a solid object was inserted into the baseline input deck to fully obstruct the flow through the passage. The revised deck was originally run for 300 seconds of simulated time. However, due to later questions (discussed subsequently) as to whether 300 seconds was sufficient to achieve nearly steady-state flow predictions, the staff performed a restart of this case to provide an additional 200 seconds of simulation time. Prior to the termination of the restart case, the FLOW-3D code displayed a run-time message stating that global parameters were essentially at steady-state conditions.

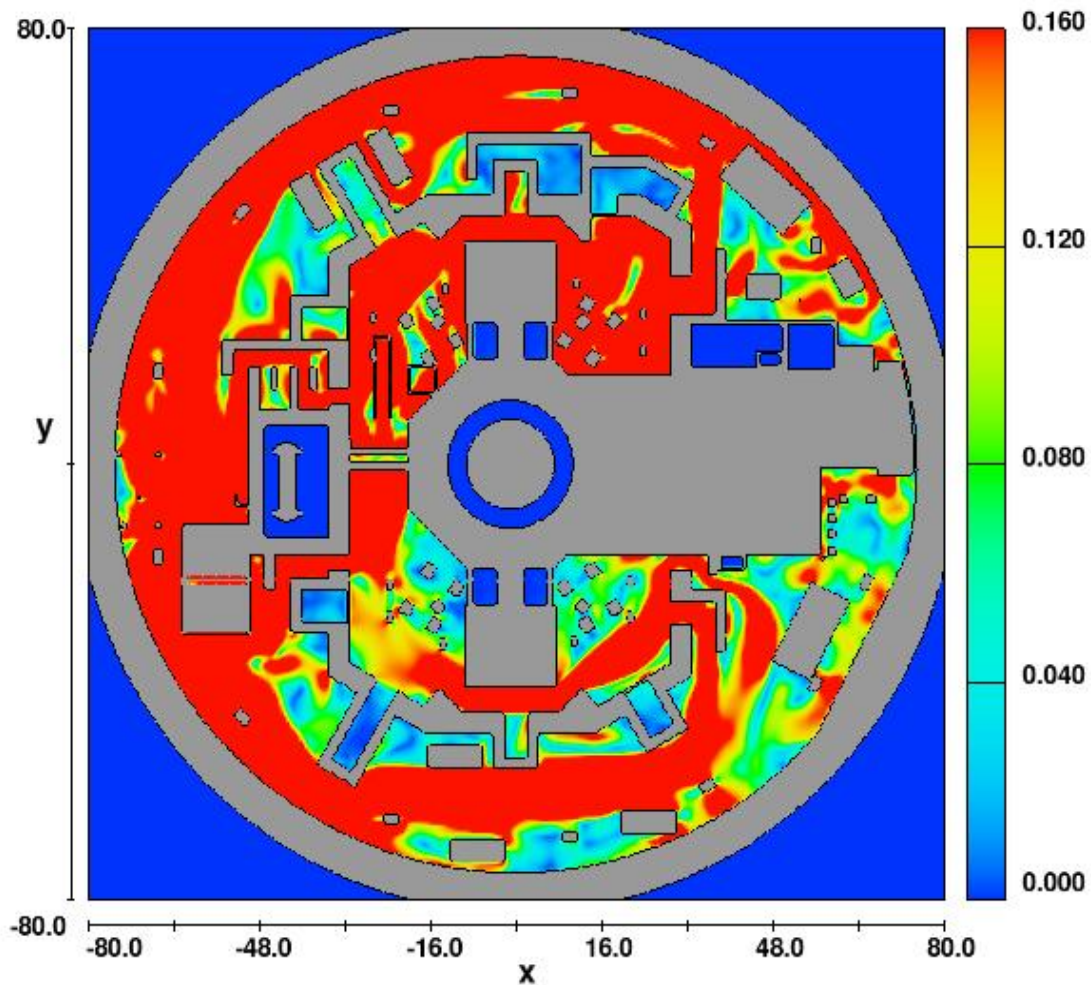


**Figure 4: Reduced Pool Temperature Case
Containment Pool Velocity [ft/s]**

A plot of the resulting velocity magnitude contours after 500 seconds of simulated time is presented as Figure 5. The blocked passage is labeled on Figure 5, which may be compared with the two preceding figures that demonstrate the flow pattern predicted for an unblocked condition.

The results of this sensitivity simulation are generally consistent with the licensee's judgment that explicitly modeling blockage at the lower southeast passage of the Loop 2 compartment would not significantly alter the containment flow field. However, by comparing the flow velocities in the southeast quadrant (i.e., lower right corner) as well as other areas of Figures 1 and 5, local perturbations are obvious. A dashed-line box is provided on Figure 5 to emphasize the most obviously perturbed local area. Other changes are also apparent, some of which were likely due to the additional 200 seconds of run time as compared to the baseline case, and which will be addressed subsequently as part of the Case 1-8 discussion.

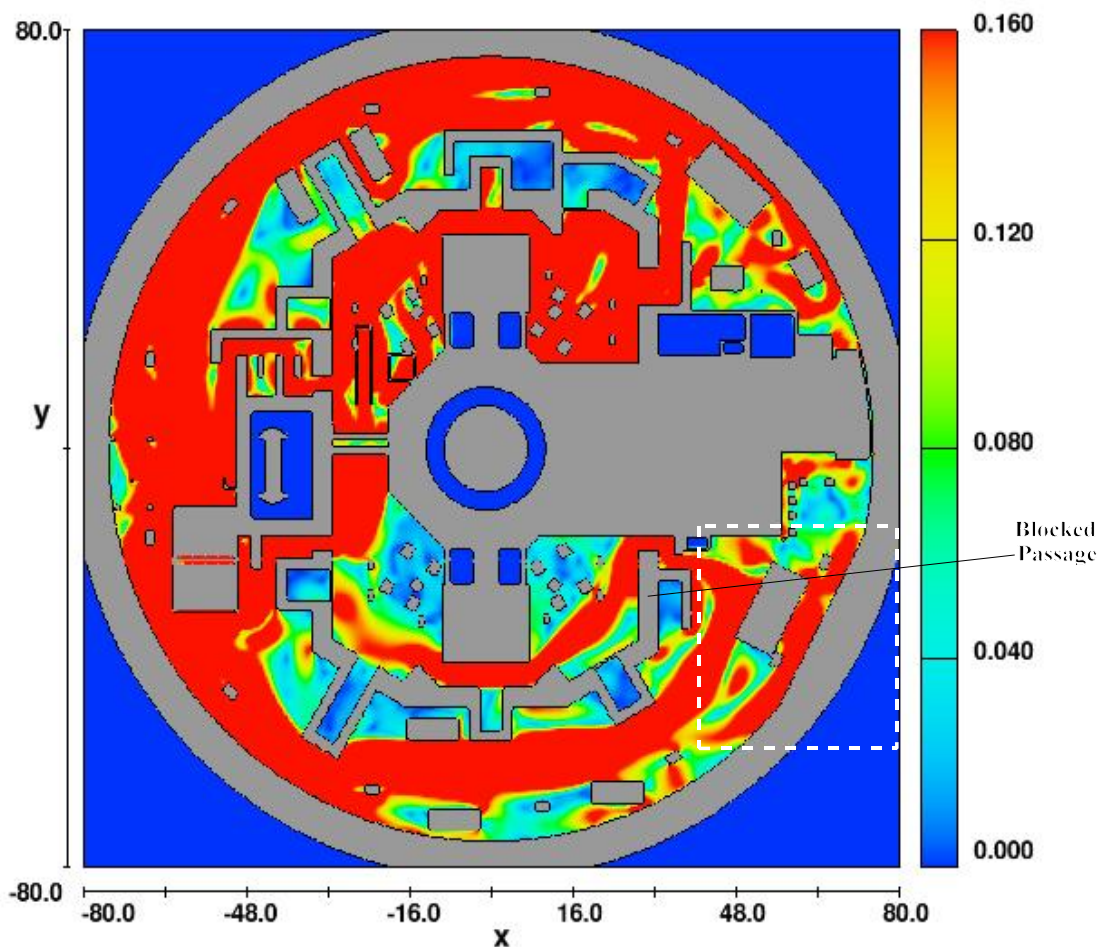


**Figure 5: Southeast Passage Blockage Case
Containment Pool Velocity [ft/s]**

Based upon SONGS-specific characteristics, including the geometric layout of the containment and analytical assumptions such as the assumed spatial distribution of debris at the initiation of sump recirculation (refer to Section 3.5.3.1 of the main report), the staff concluded that the containment pool flow field perturbations associated with this sensitivity case are not sufficient to impact the overall debris transport results for the Case 1 break. The staff further considered the potential for blockage at this passageway for Case 2 break conditions, as described subsequently in the discussion of Case 2-2 and Case 2-3.

Case 1-4: Elimination of Containment Spray Alternating Horizontal Velocity Component Case

In Section 3.5.4.1 of the main report, the staff discussed the licensee’s modeling of containment spray in the as-received CFD input decks. In particular, the staff described how the licensee modeled the introduction of spray flow into the computational domain through virtual holes “cut” in the containment floor using a velocity vector with a horizontal component having constant magnitude and a periodically alternating direction in an effort to accurately model the influx of kinetic energy to the containment pool.

The main report notes several staff concerns with the licensee's approach for modeling spray drainage that will not be repeated here. Instead, the staff performed the Case 1-4 simulation to examine the significance of the alternating horizontal component of the spray drainage velocity vector on the debris transport results by eliminating it from the CFD model and comparing the simulation results to the results of previous cases that included this feature. In particular, the staff considered this sensitivity simulation worthwhile because it could provide an indication of whether the nonrepresentative swirling horizontal velocity pattern induced above the containment floor by the containment spray drainage vector could prevent the establishment of steady, directional flow to the containment sump. The staff generated an input deck for this case by zeroing out the horizontal components of the spray drainage velocity vector from the Case 1 input deck. This case was run for 500 seconds of simulated time, with a restart at 125 seconds. Figure 6, below, plots the resulting velocity magnitude contours at 500 seconds.

A comparison of Figures 1 and 6 reveals only minor differences. The most significant of these minor differences appear to be attributable to differences in the simulation time (i.e., Figure 1 is based on a 300-second run and Figure 6 is based on a 500-second run) rather than the elimination of the horizontal component of the spray vector (which can be appreciated subsequently in the discussion of Extended Simulation Time Case, Case 1-8). One such difference is enclosed by the dashed-line box on Figure 6. The staff's comparison of Figure 1 and the Case 1-4 simulation results at 300 seconds (plot not included in this appendix) show that velocity predictions for the area within the dashed-line box are essentially equivalent. The effects of extending the simulation time will be examined in more detail in the discussion of Case 1-8.

In addition, the staff notes that the predicted flow field in the locations where containment spray is introduced to the model, particularly the regions near the containment wall on the west and south (i.e., left and bottom) of the containment pool, does not appear to be significantly affected by the removal of the horizontal velocity component (the containment spray flow addition locations for the CFD model are summarized in Section 3.5.4.1 of the main report). Based upon the assumptions made by the licensee for the spatial distribution of debris at the initiation of sump recirculation (refer to Section 3.5.3.1 of the main report), the staff concluded that the minor differences observed between Figures 1 and 6 would not appreciably impact the overall transport results.

Case 1-5: Increased Containment Spray Flow Case

In Section 3.5.4.1 of the main report, the staff noted that considerable uncertainties are associated with the licensee's assumptions and modeling of the containment spray drainage pattern in containment. In particular, the spray drainage pattern assumed by the licensee in Table 3.5-4 in the main report were derived using a methodology that appears to have significant uncertainty [1].

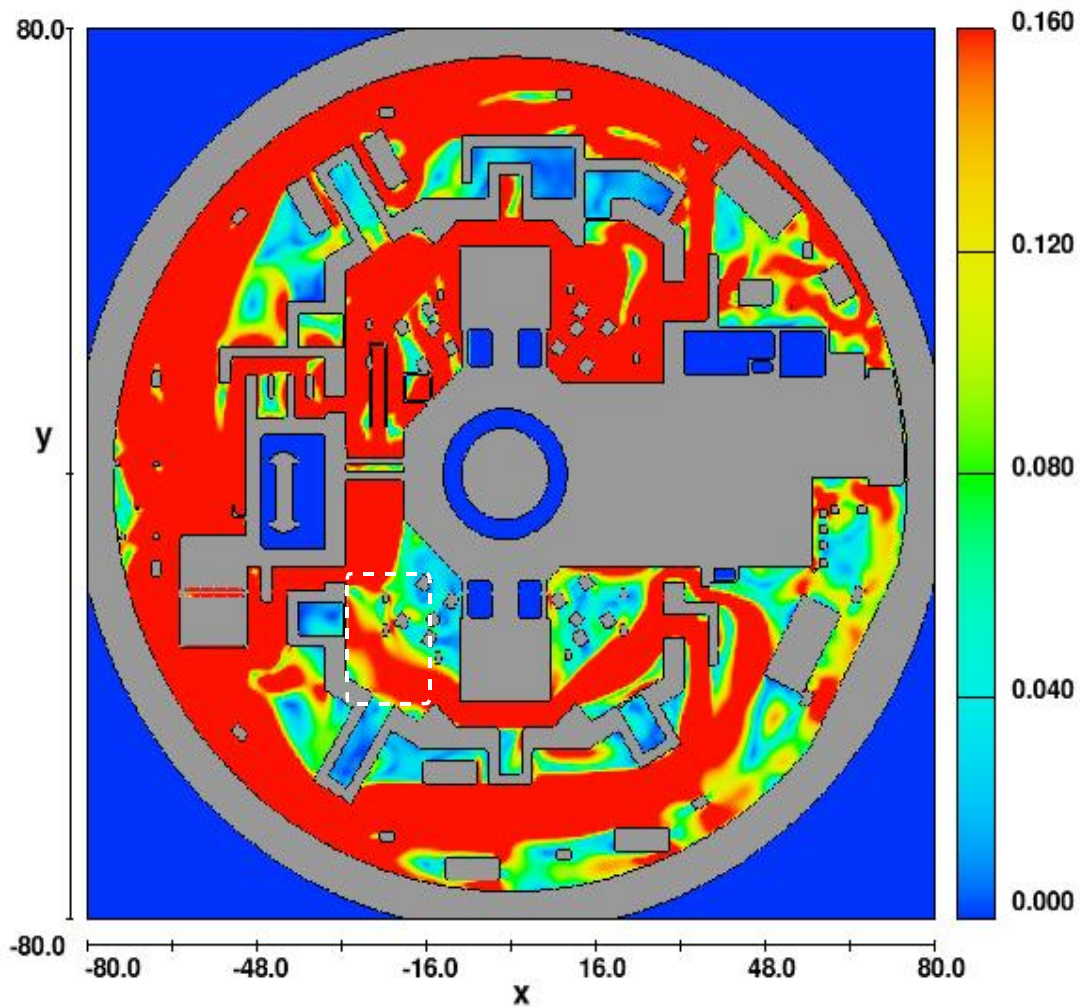


Figure 6: Elimination of Containment Spray Alternating Horizontal Velocity Component Case, Containment Pool Velocity [ft/s]

To assess the potential for uncertainties in the containment spray drainage pattern to affect the debris transport results, the staff ran a sensitivity simulation which increased the total containment spray flow by 20%, but did not alter the ratio of flows between the individual drainage locations. This simulation was run as a restart case from the 125-second run of the input deck discussed previously for Case 1-4. As such, this simulation did not include the alternating horizontal component of the containment spray flow that the licensee had implemented in the baseline case. The simulation was terminated at a simulated time of 400 seconds. A plot of the resulting containment pool velocity magnitude contours is shown as Figure 7.

As may be observed from a comparison of Figures 1 and 7, the 20% increase in total containment spray flow does not have a significant impact on the overall containment flow pattern. However, slight increases in velocity magnitude are visually apparent in several areas.

In particular, the staff focused upon one of these areas in the upper southeast quadrant of the containment pool, which is enclosed inside a dashed-line box on Figure 7.

Velocity increases within the dashed-line box on Figure 7 are of potential significance because the refueling canal drain line is located within the red-shaded area near the upper center of this box. As noted in Section 3.5.1 of the main report, 22% of washed-down debris is modeled as entering the containment pool through the refueling canal drain line. For the baseline case simulation depicted in Figure 1, it can be inferred that any small pieces of debris entering the containment pool via the refueling canal drain line would tend to settle because the velocities in this region do not exceed 0.16 ft/s (refer to the discussion of transport metrics in Section 3.5.3.2 of the main report). However, Figure 7 shows that, when the total containment spray flow is increased by 20%, the licensee's metric for tumbling transport of small pieces of mineral wool (i.e., 0.16 ft/s) is approached in the vicinity of the refueling canal drain line, although it does not appear to be exceeded along a continuous path to the recirculation sumps.

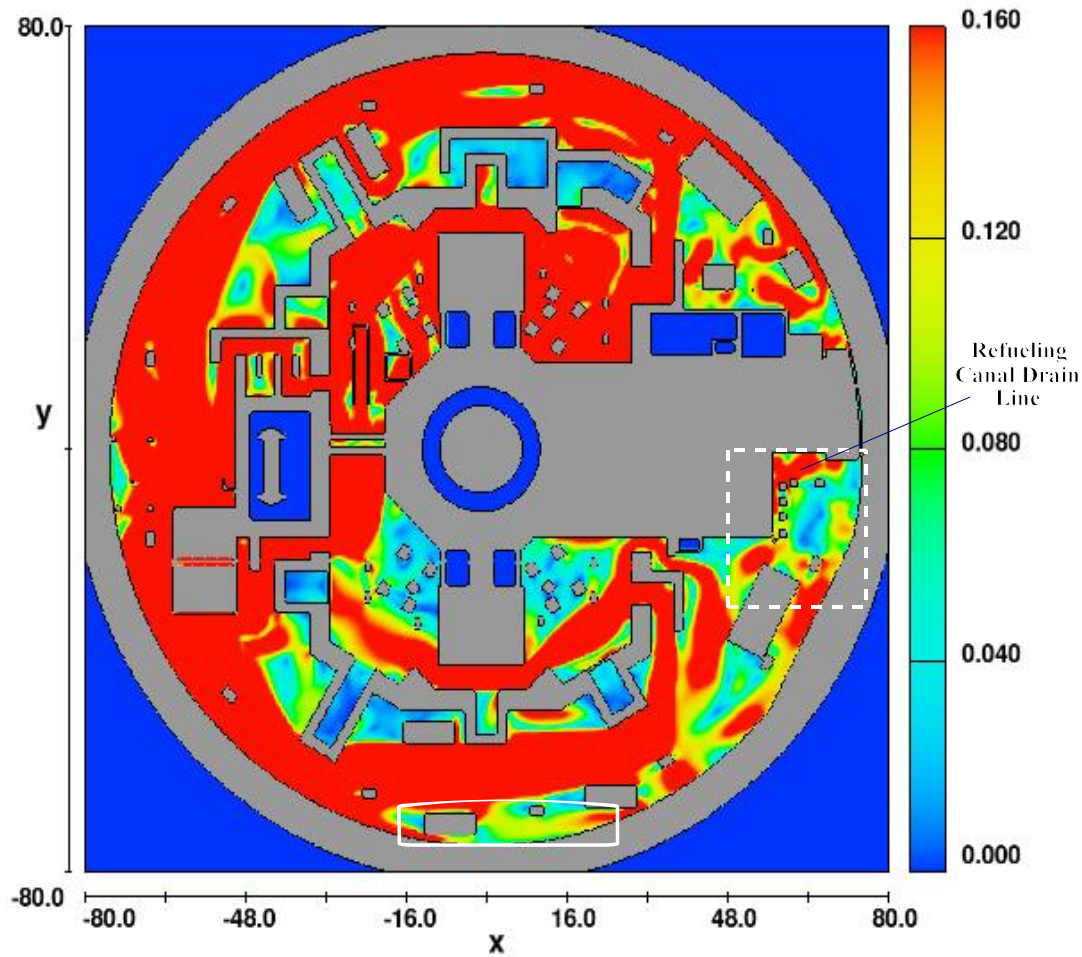


**Figure 7: Increased Containment Spray Flow Case
Containment Pool Velocity [ft/s]**

Considering the velocity increases computed for this sensitivity case, the staff decided to investigate further whether small pieces of mineral wool debris washed down through the refueling canal drain line (i.e., a total quantity of approximately 10 ft³) that the licensee's calculation considers non-transportable could actually reach the sump strainers given a credible perturbation to the spray drainage pattern. Since a 20% increase in total containment spray flow may not be credible for SONGS, the subsequent staff sensitivity simulation examines transport from the refueling canal drain area for the more credible scenario of changing the spatial distribution of the containment spray drainage flow, but maintaining the total flow rate at its baseline value.

A solid-line box is also depicted on Figure 7, which highlights an area near the south wall of the containment wherein small pieces of mineral wool debris would generally not have sufficient velocity to reach the recirculation sumps. This area is highlighted because a significant quantity of containment spray drainage and entrained washed down debris are assumed to enter the containment pool within this area, as well as the region immediately surrounding the box (refer to Sections 3.5.3.1 and 3.5.4.1 of the main report). Although the simulated increase in spray flow slightly reduced the size of the enclosed low-velocity area, due to the presence of several flow obstacles the flow field changes in this area are not sufficient to significantly affect the overall debris transport results.

Case 1-6: Increased Refueling Canal Drainage Flow Case

The previous sensitivity case assumed an increase in total containment spray flow of 20%. While this increase in total spray flow was a convenient means of identifying potential areas of the spray model for further investigation, it had the disadvantage of nonphysically increasing the overall sump flow rate as well as the velocity field throughout the containment pool. Therefore, the staff performed a follow-on sensitivity case to assess the effect of increasing the refueling canal drainage flow rate by 30% and proportionately reducing the spray flow drainage rate at the other locations (listed in Table 3.5-4 of the main report) in order to keep the total containment spray and recirculation sump flow rates equal to their baseline values. A plot of the resulting velocity magnitude contours along the containment floor is provided as Figure 8.

As expected from the results of the previous case, the overall containment flow pattern is not significantly affected by the increased refueling canal drainage flow. However, similarly to the previous results shown in Figure 7, increased local velocities are noted in Figure 8 inside the boxed area in the vicinity of the refueling canal drain line. These local velocities appear to be closely approaching the 0.16-ft/s metric at which the licensee assumed that small pieces of mineral wool can transport along the containment floor by tumbling. However, it is noted that, once again, the assumed transport metric is not exceeded along a continuous path from the refueling canal drain line to the recirculation sumps.

Based on the results of Cases 1-5 and 1-6, the staff concludes that reasonable uncertainties in the spray drainage pattern described in Section 3.5.4.1 of the main report would not likely result in a non-conservative impact on the overall debris transport results.

Case 1-7: Increased Mesh Resolution Case

The licensee employed a rectangular mesh for the computational domain in both the Case 1 and Case 2 input decks that used cells with sizes ranging from approximately 4 to 6 inches [1]. Directly above the floor, the cell height was set to 4 inches to resolve the velocity distribution in this fluid layer because this fluid layer most strongly affects the tumbling transport of debris across the containment pool floor [1]. The debris transport calculation states that the computational domain was meshed with a total of 819,200 cells [1].

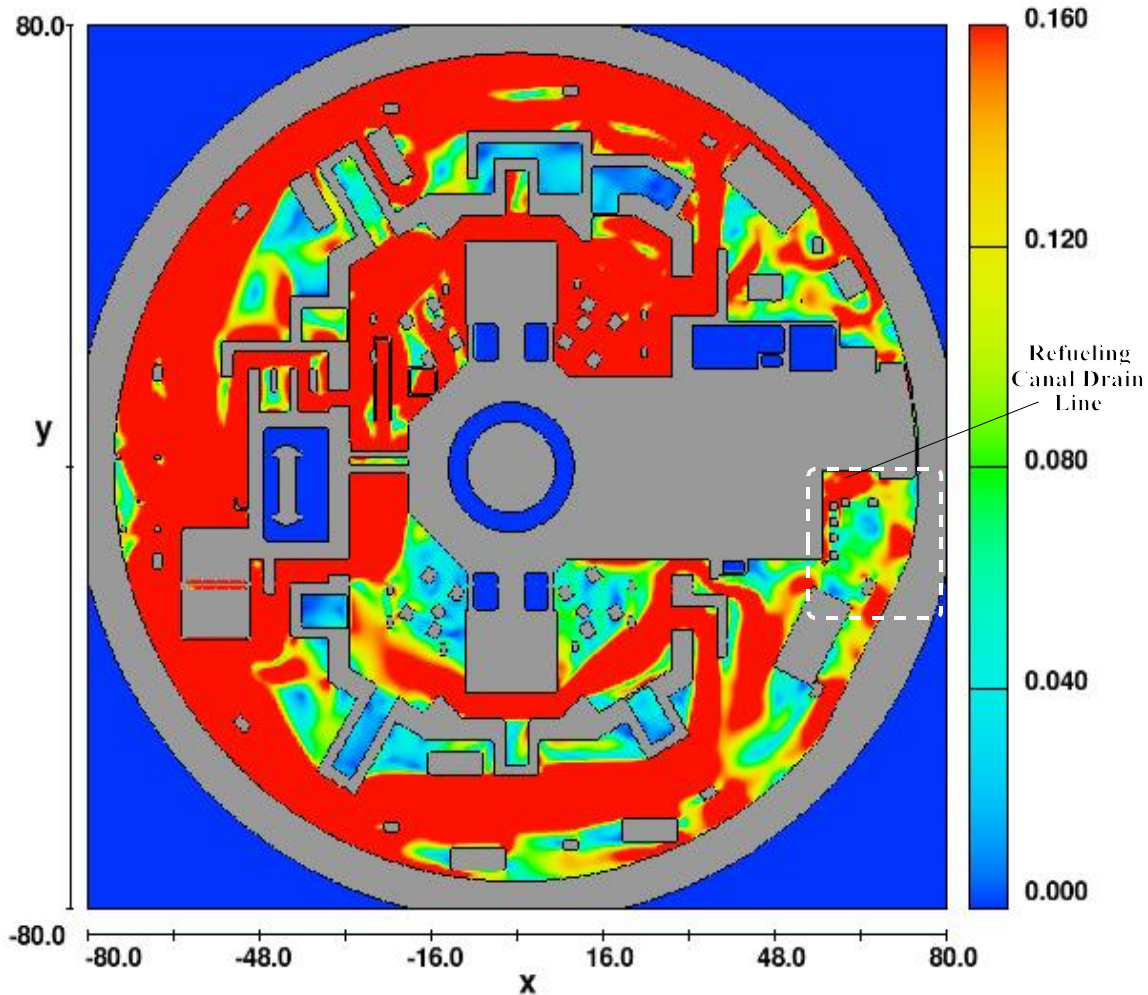


**Figure 8: Increased Refueling Canal Drainage Flow Case
Containment Pool Flow Velocity [ft/s]**

The staff performed a sensitivity case to examine the effect of increasing the total number of cells in the computational domain to determine whether an increased mesh resolution could influence the overall debris transport results. This case was run as a restart of the earlier input deck generated for Case 1-4 described above that had been run for 125 seconds.

To support this simulation, the staff revised the Case 1-4 input deck by refining the mesh to include a total of 1,470,000 computational cells. The staff increased the number of cells in the vertical direction by 66% and also added additional cells in the horizontal dimensions to avoid large aspect ratios (i.e., large differences in the lengths of the sides of computational cells) that could adversely affect the accuracy of the simulation results. The simulation was started at 125 seconds and terminated at 400 seconds of simulated time.

Subsequently, the staff decided to resolve the mesh even more finely to further improve the aspect ratio of the computational cells. Additional cells were added in the horizontal dimensions to increase the total number of computational cells to 1,732,800, which more than doubled the original number of cells used by the licensee. The simulation was performed as a restart using the results from the previous refinement to the computational mesh, being started at 400 seconds and terminated at 700 seconds of simulated time. A plot of the containment pool velocity magnitude contours at 700 seconds of simulated time is provided as Figure 9. Note that, as a result of the refinements implemented to the computational mesh, the horizontal slice of the containment pool represented is 1 inch above the containment floor, as opposed to the previous figures that were all plotted at 2 inches above the floor. (For the refined mesh, data at 2 inches was not available, but Figure 10 displays results at the 3-inch level.)

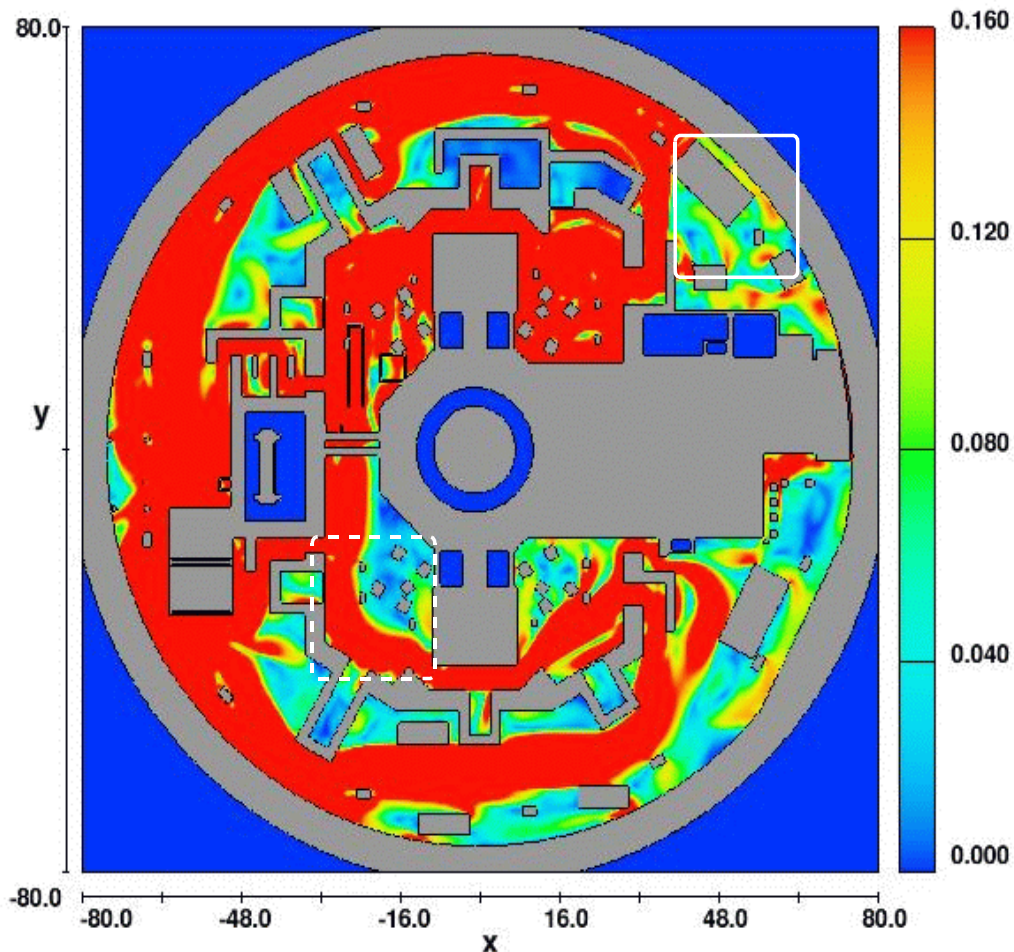


**Figure 9: Increased Computational Mesh Resolution Case
Containment Pool Velocity 1 Inch Above Floor [ft/s]**

The overall flow pattern depicted in Figure 9 is similar to that shown for the baseline results in Figure 1. However, several noteworthy differences are apparent, the most significant of which is highlighted inside a dashed-line box located on the southwest side of the Loop 2 compartment. On Figure 9, the flow within the dashed-line box appears to be concentrated along smooth streamlines hugging the outer compartment wall. In contrast, the flow in this region on Figure 1 appears diffuse and is not well-developed, presumably having been disturbed by small obstacles in the loop compartment.

A second noteworthy difference can be observed in the upper northeast quadrant of the containment pool, within the solid-line box near the containment wall. The predicted flow between the large rectangular obstacle and the containment wall is significantly reduced in Figure 9 as compared to Figure 1. Other more subtle changes in the flow pattern can also be observed for the increased mesh resolution case, particularly in areas where obstacles are present.

The differences between Figures 1 and 9 can be primarily attributed to the difference in the resolution of their respective computational meshes. In particular, the increased resolution of the mesh used to generate Figure 9 likely permitted both the containment geometry and the pool flow characteristics to be represented more accurately. However, a secondary cause of the differences is the fact that Figure 9 is based on a 700-second simulation, whereas Figure 1 was based on a 300-second simulation. The increased simulation time likely allowed the flow pattern in Figure 9 to approach steady-state conditions more closely than the baseline case. Additional examination of extending the simulation time of CFD runs is provided below in the discussion of the following sensitivity case (Case 1-8).

In order to demonstrate that the differences between Figure 1 and Figure 9 are not simply the result of their being generated at different containment pool depths, an additional containment pool velocity magnitude contour plot is provided for the increased mesh resolution case. Figure 10, below, depicts the pool velocity in a horizontal slice at a height of 3 inches above the containment floor (as opposed to the 2-inch depth used for all other containment pool flow plots except Figure 9).

Although there are several minor differences between Figures 9 and 10, these are inconsequential with respect to debris transport. This observation indicates that the differences in containment pool flow observed in Figures 9 and 10 when compared to Figure 1 are likely the result of the refined mesh (and increased simulation time), not the difference in the pool depth at which they were generated.

Based upon the assumptions made by the licensee (particularly the assumed initial spatial distribution of debris and the assumed lack of debris settling in Loop 2), the changes in the predicted containment pool flow pattern attributed to the increased mesh resolution did not lead to the identification of non-conservatism in the SONGS analysis. However, the change in the predicted flow in the southwest part of the Loop 2 compartment (highlighted again in the dashed box on Figure 10) could be important for other plant containment geometries and post-accident conditions, which demonstrates the potential significance of mesh resolution on the predicted flow pattern.

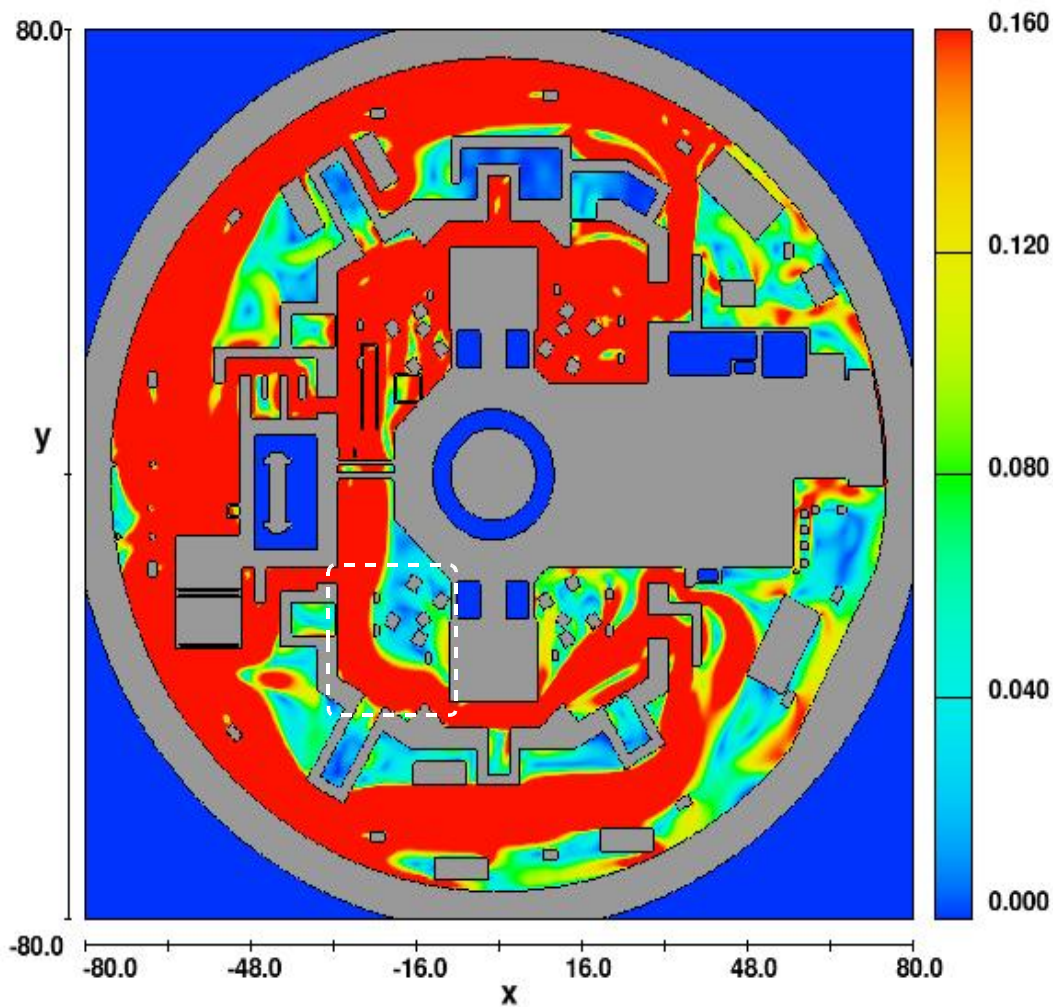


**Figure 10: Increased Mesh Resolution Case
Containment Pool Velocity 3 Inches Above Floor [ft/s]**

Case 1-8: Extended Simulation Time Case

The debris transport calculation states that the licensee ran CFD Case 1 for 300 seconds of simulation time [1]. Case 2 was run for a total of 480 seconds due to the discovery of an error in the CFD model after a 300 second run had been completed (thereupon, the code was restarted with the error corrected and run for an additional 180 seconds) [1]. The licensee stated that CFD calculations are terminated when steady-state conditions are considered to be present within the computational domain [1]. The licensee used a plot of mean kinetic energy versus time to confirm that steady-state conditions had been achieved [1]. No quantitative criteria for evaluating this plot were discussed in the transport report, and the discussion therein suggested that the determination may have been made based upon visual inspection of the plot.

To evaluate the licensee's criteria for confirming that steady-state flow predictions have been achieved by the CFD model, the staff performed several sensitivity simulations for longer time durations, including using the same input deck used for Case 1-4 (i.e., the baseline Case 1 input deck with the alternating horizontal component of the containment spray vector removed) to perform a 750-second simulation. The results of the 750-second extended simulation time case are shown below in Figure 11.

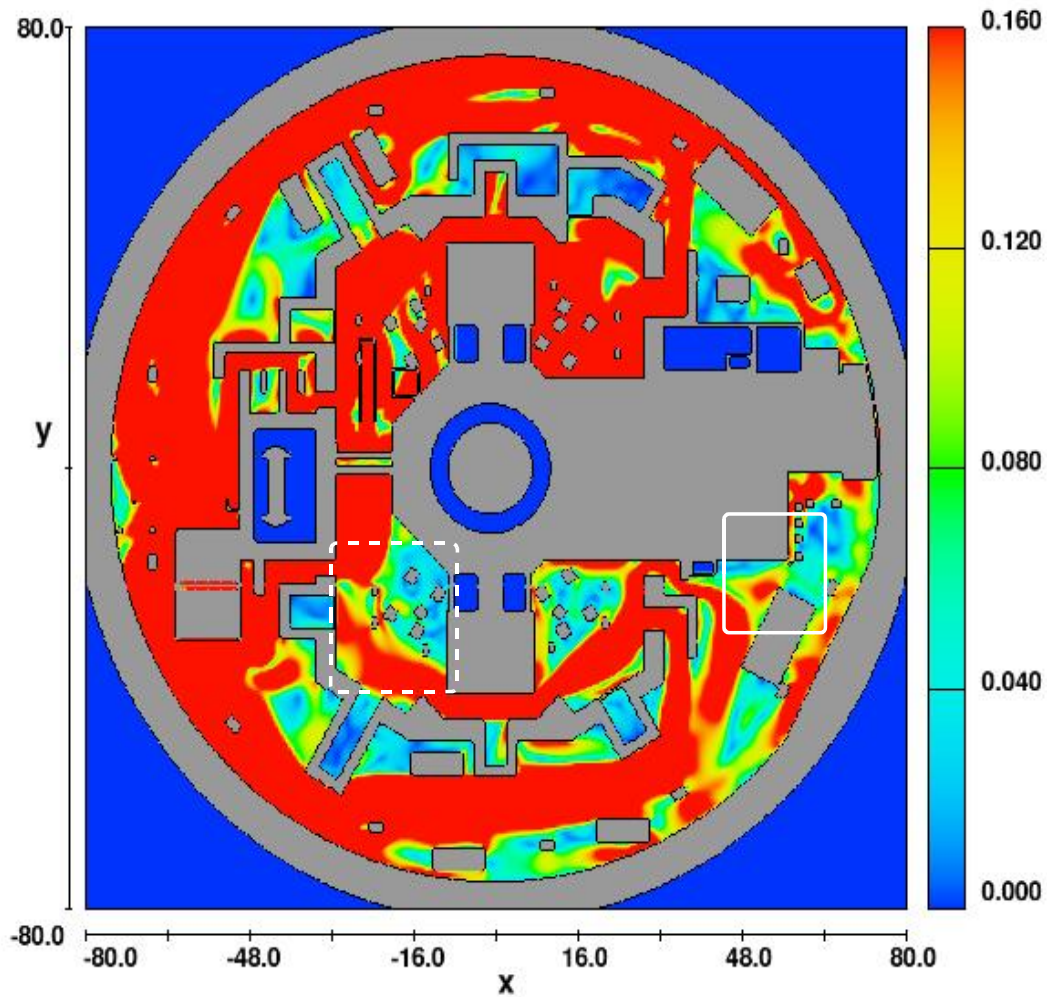


**Figure 11: Extended Simulation Time Case
Containment Pool Velocity [ft/s]**

Although earlier plots from this run are not provided in the interest of brevity, note that Figures 1 and 6 may be utilized for comparison. Although Figure 1 was run with the alternating horizontal component of the sprays activated, this feature does not significantly influence the resulting velocity field; thus, Figure 1 essentially represents the Case 1-8 simulation at 300 seconds. Figure 6 shows a run of the same input deck used for Case 1-8 at 500 seconds of simulated time. Thus, the temporal progression of the extended simulation time calculation can be observed by comparing Figures 1, 6, and 11.

While, once again, the global flow pattern in containment is not significantly affected by the increased simulation time, several interesting changes to the flow field can be noted. Two of the most notable changes with respect to the debris transport analysis are highlighted on Figure 11. First, the dashed-line box on Figure 11 shows the velocity magnitude contours in the southwest corner of the Loop 2 compartment at a simulated time of 750 seconds. Figure 6 displays a velocity field of similar magnitude in this local region at 500 seconds. In contrast to these two plots, Figure 1 shows significantly lower velocities in this region at 300 seconds of simulated time. The comparison of these figures suggests that the velocity field in the southwest corner of the Loop 2 compartment has not been fully resolved at 300 seconds. This observation is further confirmed by sequentially examining several of the velocity magnitude contour plots for the three cases prior to 300 seconds (not shown in this appendix), which clearly indicate that the flow in this region is still rapidly developing. It is also noted that the area within the dashed-line box was previously examined on Figure 9, which presented the results of the increased mesh resolution case. By comparing Figures 9 and 11, the impact of the refined mesh can be appreciated in comparative isolation because the slight difference in run time for these two cases is not expected to have a significant impact on the simulation results.

The second noteworthy observation from Figure 11 is highlighted by the solid-line box in the southeast quadrant of the containment. This figure shows that, at 750 seconds of simulated time, the velocity field in the vicinity of the refueling canal drain line appears to be approaching the threshold at which some small pieces of mineral wool washed-down through the drain line could be transported to the recirculation sumps via tumbling. Note that the predicted flow field in Figure 11 for this region contrasts with that of Figure 1, which appears to indicate that small pieces of mineral wool washed down through the refueling canal drain would be highly unlikely to reach the recirculation sumps. Further consideration of Figure 6 indicates that, unlike the flow in the southwest corner of the Loop 2 compartment discussed above, the flow field in the region enclosed by the solid-line box has not completely developed, even at 500 seconds.

The two observations discussed above suggest that, while terminating CFD simulations based upon visual indications of mean kinetic energy versus time plots may be adequate for determining that a steady global containment pool flow pattern has been established, this criterion alone may not be generally adequate for concluding that predictions of localized flows with potential significance to the overall debris transport results have reached nearly steady-state conditions. (Recall that, as demonstrated by Figures 2 and 3, both the estimated mean kinetic energy and average turbulent kinetic energy had appeared relatively stable after a simulation time of 300 seconds for the baseline case.) As may be inferred from the observations cited above, local regions where the achievement of steady-state flow conditions may require additional time can often include areas where obstacles or constrictions are present, which tend to complicate predictions of the flow field. The staff found that using the FLOW-3D output files to examine of the progression of the CFD solution at various times prior to the simulation termination was useful in evaluating whether sufficient convergence had been achieved in local areas of potential importance to the debris transport results.

Despite this general concern with the licensee's methodology for terminating CFD simulations, the staff did not consider the SONGS debris transport results to be non-conservative because (1) debris settling was not credited in the southwest corner of the Loop 2 compartment where velocities were underpredicted in the baseline case and (2) staff sensitivity simulations, including Case 1-5 (Increased Containment Spray Flow Case), Case 1-6 (Increased Refueling

Canal Drainage Flow Case), Case 1-7 (Increased Mesh Resolution Case), and Case 2-3 (Southeast Passage Blockage Plus Increased Refueling Canal Drainage Flow Case) provide assurance that small pieces of mineral wool washed down through the refueling canal drain line are unlikely to transport to the recirculation sumps.

Case 2-1: Elimination of Containment Spray Alternating Horizontal Velocity Component Case

As described above in the discussion of Case 1-4, the licensee introduced containment spray flow into the computational domain through holes cut in the containment floor using a velocity vector with a horizontal component having constant magnitude and a periodically alternating direction, in an effort to accurately model the influx of kinetic energy to the containment pool. Section 3.5 of the main report notes several staff concerns with this approach that will not be repeated here.

The staff performed this sensitivity case to examine the effect of eliminating the alternating horizontal component of the velocity vector for the incoming spray on the debris transport results for the Case 2 break. As for Case 1-4, the staff accomplished this objective by modifying the baseline input deck by zeroing out the horizontal components of the spray velocity vector. This case was run for 500 seconds of simulated time. Figure 12, below, plots the resulting velocity magnitude contours.

Note that the overall containment flow pattern for the Case 2 break location is somewhat different from that caused by the Case 1 break. For reference, labels for the break location, the refueling canal drain line, and the recirculation sumps are provided on Figure 12, as well as arrows to highlight the general pattern of the containment pool flow. These arrows should not be considered to be vectors, since no attempt has been made to scale their length based upon the local velocity of the flow. As expected, the general direction of the containment pool flow is from the break location and refueling canal drain toward the recirculation sumps.

The staff noted that the containment pool velocity magnitude contours displayed on Figure 12 are very similar to those depicted in the corresponding figure in the licensee's debris transport calculation, Figure 5.9.29 [1]. Several minor differences were noted between the two figures, none of which appeared to have significant implications with respect to the debris transport results. Note also that slight differences are expected between Figure 12 and Figure 5.9.29 [1] as a result of the difference in the run times for the two cases and possibly the staff's input deck modification that removed the horizontal component of the containment spray vector.

Similar to the discussion for Case 1-4, the staff noted that the predicted flow field in the locations where containment spray is introduced to the model, particularly the regions near the containment wall on the west and south (i.e., left and bottom) of the containment pool, does not appear to be significantly affected by the removal of the alternating horizontal velocity component. As a result of this observation, the staff concluded that the presence of the alternating horizontal component of the spray vector did not appear to significantly influence the overall debris transport results for either the Case 1 or the Case 2 break.

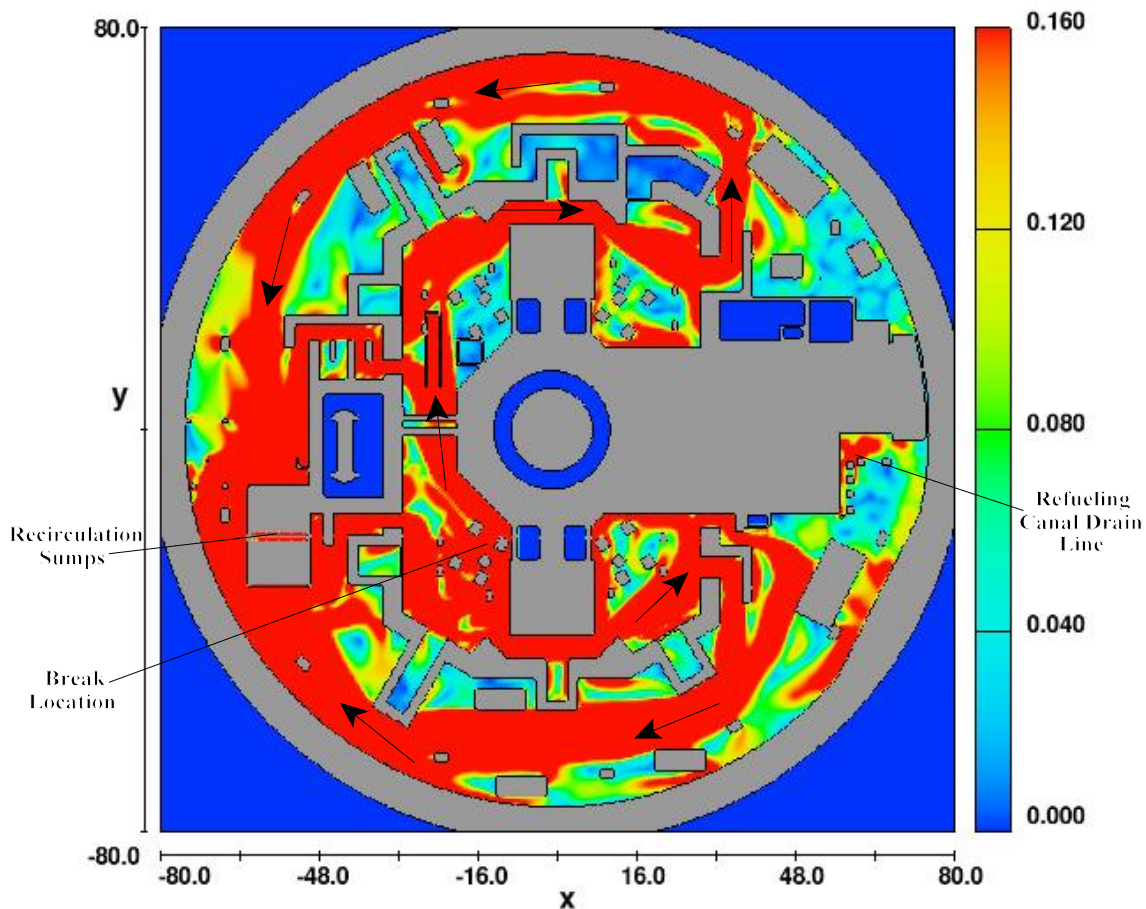


Figure 12: Elimination of Containment Spray Alternating Horizontal Velocity Component Case, Containment Pool Velocity [ft/s]

Case 2-2: Southeast Passage Blockage Case

As described earlier in the discussion of Case 1-3, the licensee noted that a HVAC plenum located in the southeast corner of the Loop 2 steam generator compartment poses a potential flow blockage point. The licensee did not model this blockage in its Case 1 or Case input deck based upon engineering judgment that the presence of another open passageway in the same general location would preclude significant changes to the CFD simulation results [1].

Although explicitly modeling the effect of blockage in the affected passage did not appear to result in any changes affecting the overall debris transport results for the Case 1 break location, the staff considered it important to assess this issue for the Case 2 break location as well due to the apparent flow increase through the southeast passages of the Loop 2 compartment that would occur for the Case 2 break. To implement the blockage model in FLOW-3D, the staff inserted a solid object into the Case 2 input deck to fully obstruct the flow through the lower southeast passage of the Loop 2 compartment.

The revised deck was run as a restart case using the results of the previous simulation, Case 2-1. Thus, as for Case 2-1, the simulation of Case 2-2 was performed with the alternating horizontal velocity component of the spray drainage vector zeroed out. The simulation was begun at 350 seconds and run until a simulated time of 500 seconds was reached. To ensure that steady-state flow had been achieved throughout the containment pool, this case was subsequently restarted at 500 seconds and run until a simulated time of 650 seconds was reached. Just prior to the termination of the simulation, the FLOW-3D code displayed a run-time message stating that global parameters were essentially at steady-state conditions.

A plot of the resulting velocity magnitude contours is presented below as Figure 13. The blocked passage is labeled.

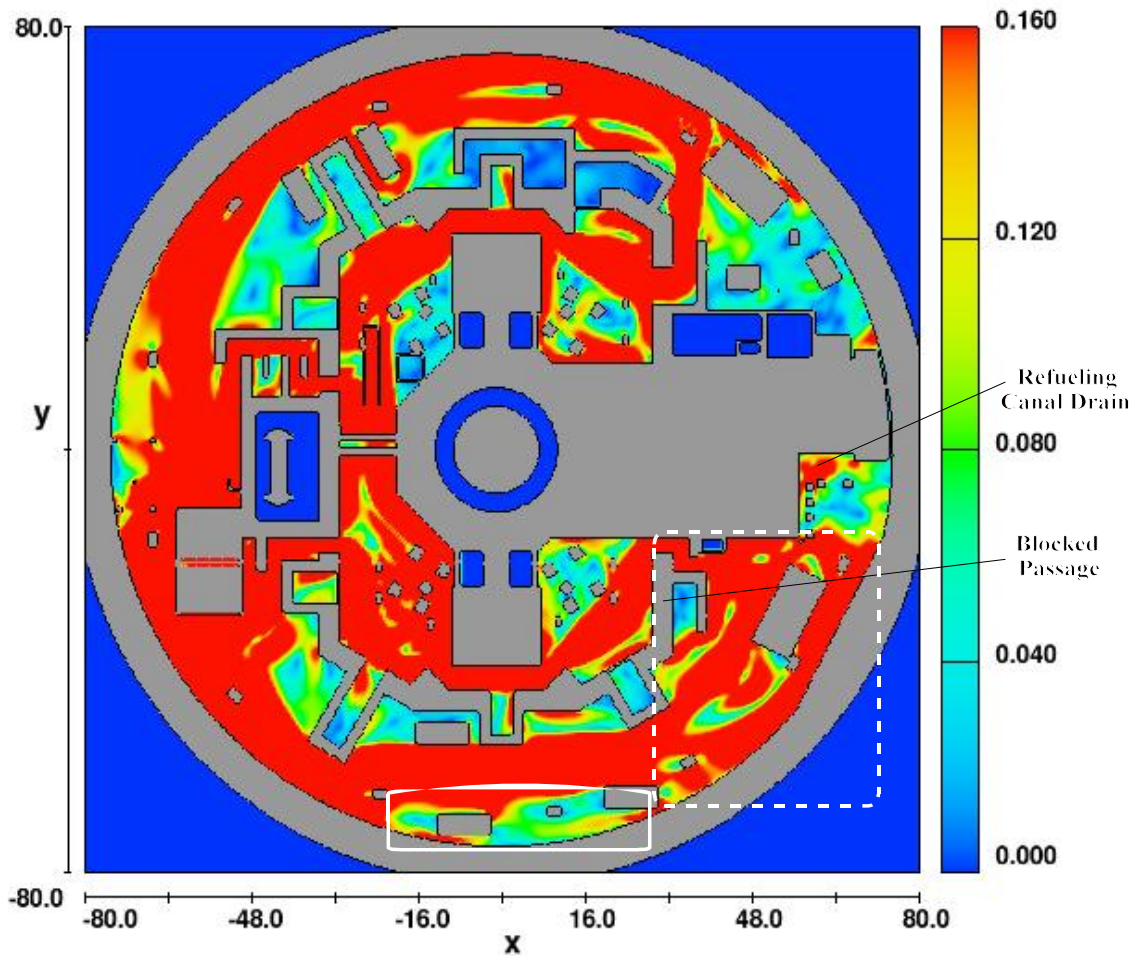


**Figure 13: Southeast Passage Blockage Case
Containment Pool Velocity [ft/s]**

While the overall flow pattern in Figure 13 is similar to that of Figure 12 (which essentially serves as the baseline case for the Case 2 break), the flow velocities in a substantial portion of the southeast quadrant of the containment pool (highlighted in a dashed-line box on Figure 13)

appear to be increased by the explicit modeling of blockage at the lower southeast passage. Prior to running the simulation, the staff was concerned that these increased velocities could lead to additional transport of debris washed down through the refueling canal drain and along the south containment wall (highlighted in a solid-line box on Figure 13). However, Figure 13 indicates that local changes in the flow velocity do not significantly impact the refueling canal drain line area or the size of the low-velocity zone along the south containment wall.

Based upon the initial debris spatial distribution assumed by the licensee (refer to Section 3.5.3.1 of the main report), the flow velocity increases in the southeast quadrant do not significantly affect the overall debris transport results. However, the extent of the velocity increases shown in the southeast quadrant of Figure 13 could not have been fully appreciated prior to running the simulation. Therefore, while these perturbations were not ultimately significant for either the Case 1 or Case 2 SONGS input decks, their order of magnitude suggests that the area-based methodology used for computing debris transport fractions (this methodology is described in Section 3.5.4.2 in the main body of this report) could yield non-conservative results if applied in a similar manner to geometric and analytical conditions that may exist for other plants.

Case 2-3: Southeast Passage Blockage Plus Increased Refueling Canal Drainage Flow Case

The results of the staff's separate sensitivity simulations for modeling blockage in one of the southeast passages of Loop 2 (Case 1-3 and Case 2-2) and for modeling increased refueling canal drainage flow (Case 1-5) indicated that the containment pool velocity field could be approaching the threshold at which a fraction of the small pieces of mineral wool washed down through the refueling canal drain line might transport to the recirculation sumps. As a result, the staff investigated whether the combination of the two circumstances could lead to significant transport of the small pieces of mineral wool debris washed down through the refueling canal drain line.

This sensitivity case was implemented by performing modifications to the Case 2 input deck using the techniques described above for modeling blockage and for altering the distribution of the containment spray flow. As in Case 1-5, the refueling canal drain line flow was increased by 30% and a proportionate flow decrease was implemented to the other areas affected by containment spray to ensure that the baseline containment spray flow rate was maintained. The simulation was run as a restart case using results previously generated with the Case 2-2 input deck, being started at 500 seconds and terminated at 800 seconds. The resulting velocity magnitude contours are displayed in Figure 14.

A comparison between Figures 13 and 14 reveals relatively minor differences when a 30% increase in the refueling canal drainage flow is explicitly considered. A dashed-line box on the east side of the containment near the refueling canal drain line shows one area where velocity increases are noticeable but not on the verge of continuously exceeding the 0.16-ft/s tumbling transport metric for small pieces of mineral wool. The solid-line box against the south wall of the containment shows that significant changes were similarly not predicted in the enclosed low-velocity region.

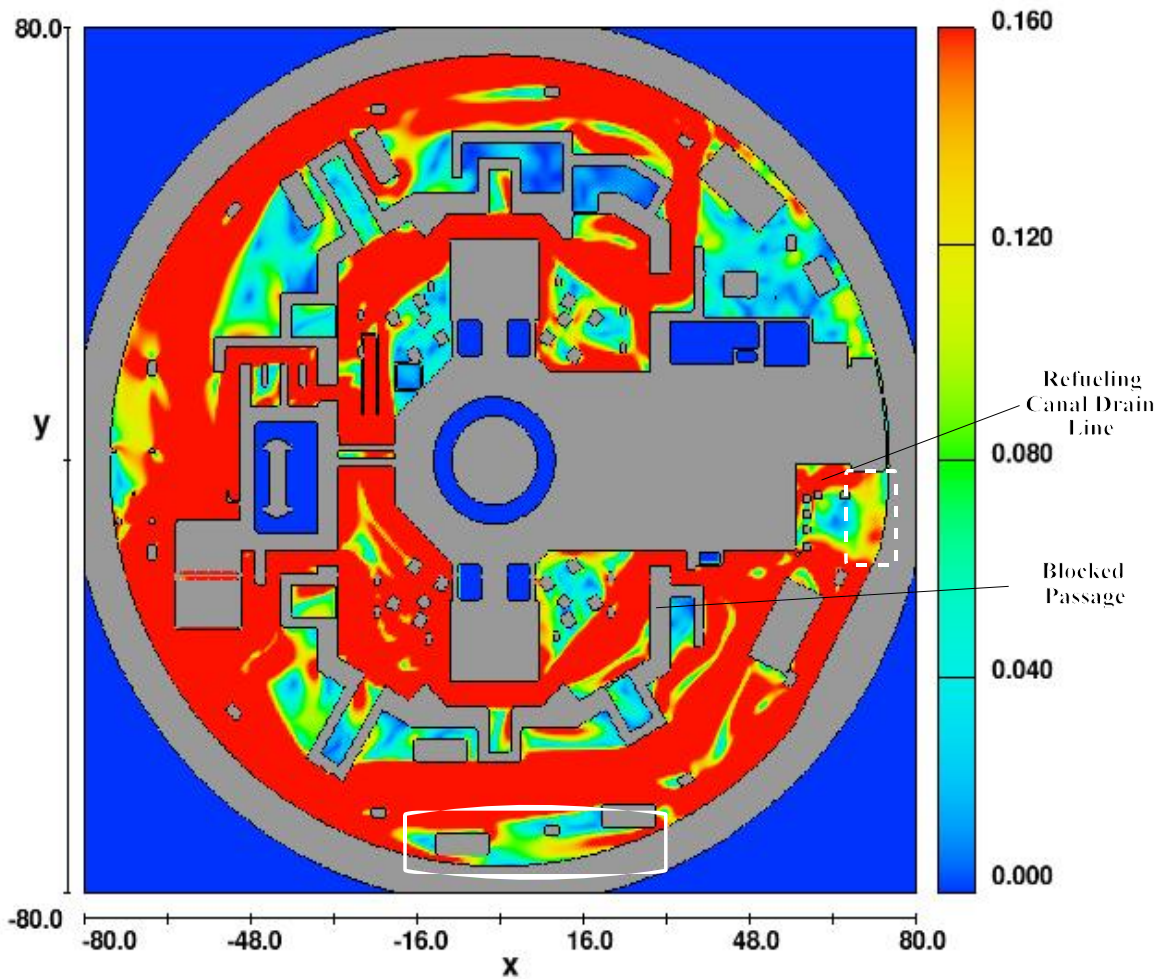


Figure 14: Southeast Passage Blockage Plus Increased Refueling Canal Drainage Flow Case, Containment Pool Velocity [ft/s]

Based upon the results of this sensitivity simulation, the staff has confidence that small pieces of mineral wool washed down through the refueling canal drain line would not transport to the recirculation sumps and that the licensee’s transport analysis is relatively robust in the face of credible perturbations to the CFD model.

Additional Simulation of Concentrated Containment Spray Drainage

The staff performed one final CFD simulation to investigate the potential effect that concentrated, continuous drainage of containment sprays (as opposed to the dispersed droplet spray flow modeled in the licensee’s CFD input decks) might have upon the flow field within the SONGS containment pool. The basis for performing this simulation was that, as described further in Section 3.5.4.1.2 of the main report, the staff was concerned that concentrated spray drainage (e.g., cascading miniature “waterfalls” of runoff from solid surfaces in containment) would likely occur in localized areas of the containment pool. The staff considered that

concentrated spray drainage could have a non-conservative impact upon flow velocity, turbulence, and the erosion of washed-down debris in local areas of the containment pool exposed to containment spray drainage. By performing this CFD simulation, the staff intended to gain order-of-magnitude insights in determining the potential impact of explicitly modeling concentrated containment spray drainage.

The construction of a detailed model of containment spray drainage at SONGS was prevented by several constraints, including (1) a lack of detailed geometric information, (2) a lack of computational resources, and (3) a lack of time to develop the computational model. Under these constraints, the staff developed a simplified model of flow falling off a ledge and into a pool of water. The size of the computational domain for this problem was a small fraction of the total containment pool volume (i.e., several hundred cubic feet).

The staff's simplified model placed a fluid mass source atop a solid floor approximately 11 ft above the surface of a pool having an initial depth of approximately 1.6 ft (however, the depth was allowed to increase with time to examine pool depths of up to approximately 3–4 ft). The flow from the mass source was allowed to spread across a solid floor. Upon reaching the edge of the floor, the flow then fell through open space and entered the pool of water below. The flow rate of the mass source was scaled and varied in an attempt to ensure that expected spray drainage conditions would be bounded. A number of aspects of the staff's model proved challenging, including generating an adequately refined mesh for resolving the stream of water falling into the pool and minimizing the artificial and disproportionate influence of boundary conditions on this relatively small computational domain.

However, despite the difficulties and limitations described above, the results of the simulation indicated that concentrated, continuous streams of spray drainage may have the capacity to stir up debris at the bottom of a pool that is on the order of several feet deep.

Considering that the licensee assumed that a fraction of the debris entrained in the spray drainage flow would settle in low-velocity zones along the containment periphery (e.g., the area boxed in by a solid line on Figures 7, 13, and 14), the results of this simulation suggest that a more conservative modeling of the containment sprays in these zones is necessary to ensure that such credit is reasonable. As noted in Section 3.5 of the main report, the licensee's modeling of containment spray drainage as a dispersed flow is **Open Item 6**.

Summary

The staff performed a series of sensitivity simulations based upon the CFD input decks provided by the licensee for the Case 1 and Case 2 break locations. The objective of the sensitivity simulations was to verify that credible perturbations to assumptions and modeling conditions used in the licensee's CFD calculations would not significantly affect containment pool flow parameters of importance to debris transport, such as velocity and turbulence. Overall, the staff's sensitivity simulations found the licensee's debris transport results to be relatively robust when credible perturbations were applied to the input assumptions used in the CFD model. However, several instances were cited where the general methodology used by the licensee may result in non-conservatism if applied in a similar manner to different conditions at other plants, the most significant of which were the lack of an explicit model for blockage points and the termination of CFD cases prior to establishing steady-state local flow

conditions.

The staff's simplified model of concentrated, continuous spray drainage supports **Open Item 6** in Section 3.5 of the main report stating that the licensee should provide additional justification for its position that containment spray may be conservatively modeled as a dispersed flow.

Reference

1. T. Sande, "San Onofre Units 2 and 3 GSI-191 Containment Recirculation Sump Evaluation: Debris Transport Calculation," Calculational Report, ALION-REP-SONGS-2933-003, Rev. 2, January 9, 2006.